

Realization of broadband terahertz reflector by all-dielectric monolayer grating

BO FANG^a, SHUANG HAN^b, JINGWEN XIE^b, CHENXIA LI^{b,*}, ZHI HONG^c, XUFENG JING^{b,c,#}

^aCollege of Metrology & Measurement Engineering, China Jiliang University, Hangzhou 310018, China

^bInstitute of Optoelectronic Technology, China Jiliang University, Hangzhou 310018, China

^cCentre for THz Research, China Jiliang University, Hangzhou 310018, China

We exploit Mie resonances in all-dielectric grating metamaterials to design a single-negative all-dielectric near-perfect reflector. The average reflection over 99.9% at single frequency in terahertz region is achieved. Ultrabroadband perfect reflector was proposed by all dielectric single-layer super cell grating metamaterial structure. It consists of two Silicon grating strips with different width in single unit cell, which possesses peak reflection over 99.9% and a near-perfect reflection band of 0.79THz from 1.19THz to 1.98THz, surpassing the reflectance of metallic mirrors. The coupling effect of Si grating elements with different width is revealed by magnetic and electric dipole Mie resonances. The physic mechanism of broadband perfect reflection is disclosed by the electromagnetic field distribution of super cell grating. Polarization effect of perfect reflection is also studied. The proposed super cell metamaterial structure can be potentially applied to other photonic devices to realize broadband effect.

(Received September 11, 2018; accepted April 8, 2019)

Keywords: Grating, Reflector, Terahertz

1. Introduction

Metamaterials (MMs) are artificial media with subwavelength scale, which exhibit unique properties [1-4], such as negative refraction index [5], invisible cloak [6], sub-diffraction-limited imaging [7], and perfect reflection [8]. In these applications, the perfect reflectors are widely used as optical devices for controlling light propagation. Traditionally, perfect reflectors have been formed using metal-based unit cells, in which conduction current is used to realize magnetic and electric resonances for manipulating the effective permeability and permittivity [9-11], respectively. But these MMs properties have been limited primarily by the absorption loss and fabrication complexity associated with the metallic elements [10-12], especially at optical band. For instance, some gold and silver mirrors exhibit high reflection with still absorptivity of 2% in telecommunication band [13,14]. Moreover, metallic plasmonic MM reflectors often exhibit complicated geometries [2,3], which limit some potential mass production applications. Even though Bragg reflectors (DBRs) with alternating multiple dielectric layers were proposed as an alternative of metallic reflectors, but the deposition of dielectric layers for Bragg reflectors leads to a lengthy process [15].

In order to overcome these problems, researchers have focused on using all-dielectric MMs to achieve perfect reflector similar to their metallic reflector. For example, R. Magnusson et al. exploited Mie resonance of an array of

dielectric grating to obtain a bulk magnetic and electric response to achieve perfect reflector [16]. Since then, a number of researchers are interesting in measured and predicted reflectivity spectra from thin layer of all dielectric MMs. By controlling electric and magnetic resonances separation, MMs can be able to realize perfect reflector in which either the permittivity ϵ or permeability is less than zero. In recent research, Slovick et al. [17] proposed a single-negative all-dielectric MM possessing broadband near perfect reflection at optical frequencies. Moitra et al. [18] demonstrated a 100 nm near-perfect reflectance band of MMs by using Si cylinder resonators in the telecommunication band. Compared with these systems in the telecommunication band, ultrabroadband perfect reflectors would be useful in bio-imaging and nanosensing [19,20], laser cavities and so on [17].

In this study, based on general grating structure that can not realize broadband perfect reflection, we propose a monolayer super cell grating MM to realize ultrabroadband perfect reflector in terahertz region. We used Si dielectric grating because it can control spectral separation of the electric and magnetic Mie resonances by changing the grating geometry easily. And the electromagnetic radiation can be confined into standing waves or resonant modes (electric or magnetic mode) in gratings [21,22]. Furthermore, in order to realize an ultra-wideband reflector, we compared the reflection of a single Si element in unit cell of grating and two Si elements with different width in super cell, respectively. It

can be revealed that the single-layer super cell grating MM with two elements in unit cell can achieve ultrabroadband perfect reflector in near-perfect reflection band of 0.79THz with reflection (>99%). Also, we attempt to realize broadband perfect reflector by using super cell grating MM with three elements in unit cell. In order to disclose the insight of broadband perfect reflector, the effective constitutive parameters were extracted, and the electromagnetic field distribution with Mie resonances was numerically simulated.

2. Theoretical conditions of perfect reflection

For a semi-infinite medium, it can be shown that the amplitude reflectance coefficient r and reflection R at normal incidence from [23] vacuum are

$$r = r_0 e^{i\varphi} = \frac{z-1}{z+1} \quad (1)$$

$$R = |r|^2 = \frac{(z'-1)^2 + z''^2}{(z'+1)^2 + z''^2} \quad (2)$$

$$z = z' + z''i = \sqrt{\frac{\mu}{\varepsilon}}, \quad \mu = \mu' + \mu''i \quad (3)$$

$$\varepsilon = \varepsilon' + \varepsilon''i \quad (3)$$

where r_0 and φ are the reflectance amplitude and phase, z is the complex impedance. The perfect reflection of all-dielectric grating MM can be realized when the real part of the impedance (z') of the effective medium is zero. When the impedance is $z'=0$, the perfect reflection conditions can be expressed as

$$\frac{\varepsilon'}{\mu'} < 0 \quad (4)$$

$$\varepsilon''\mu' - \mu''\varepsilon' = 0 \quad (5)$$

The first condition in Eq. (4) requires the real parts of the permittivity and permeability have opposite signs [24,25]. Furthermore, the second condition in Eq. (5) is satisfied in lossless materials. In order to achieve near-perfect reflection with a finite thickness medium slab composed of absorbing constituents, the condition on the impedance ($z'=0$) is as that of lossless material, but the imaginary part of the index (n'') must be maximized to prevent evanescent tunneling across the slab [14,25]. Although Eqs. (4) and (5) are useful from a conceptual point of view, Eq. (5) is not satisfied for realistic materials with absorption. So when the impedance is sufficiently close to zero, all-dielectric MMs reflector can be realized with arbitrarily high reflection.

A standard S-parameter retrieval algorithm can be used to extract the effective permittivity and permeability of all dielectric grating MM [25, 26]. We characterize the grating MM structure as an effective homogenous slab under the condition of a long wavelength. S parameters for a plane wave incident normally on the slab of grating are represented as [27]

$$S_{11} = r(1 - e^{i2nk_0h}) / (1 - r^2 e^{i2nk_0h}) \quad (6)$$

$$S_{21} = (1 - r^2) e^{ink_0h} / (1 - r^2 e^{i2nk_0h}) \quad (7)$$

where $r=(z-1)/(z+1)$ is the half space reflectance coefficient, z is the impedance, n is the refractive index. By inverting Eqs. (6) and (7), the impedance z and the refractive index n can be respectively expressed by

$$z = \pm \sqrt{[(1 + S_{11})^2 - S_{21}^2] / [(1 - S_{11})^2 - S_{21}^2]} \quad (8)$$

$$e^{ink_0h} = X \pm i\sqrt{1 - X^2} \quad (9)$$

where $X = (1 - S_{11}^2 + S_{21}^2)$. From Eq. (9), the effective refractive index can be determined by

$$n = \frac{1}{k_0h} \left\{ \left[\ln(e^{ink_0h}) \right]' + 2m\pi \right\} - i \left[\ln(e^{ink_0h}) \right]'' \quad (10)$$

where m is an integer related to the branch index of n' . For a passive medium, the solved z should obey the condition as $z' \geq 0$, where $(\cdot)'$ and $(\cdot)''$ indicate the real part and imaginary part operators, respectively. For above retrieval process, Eqs. (8) and (10) can be directly used to determine effective refractive index and impedance [24]. The permittivity ε and permeability μ can be calculated by $\varepsilon=n/z$ and $\mu=nz$ for the all-dielectric grating MM.

3. Broadband perfect reflector of grating MM

The single-layer 1D dielectric unit cell of the common grating is shown in Fig. 1(a). The incident terahertz wave is along z direction, the period of grating is P with grating line width x and thickness h . The dielectric grating material is silicon, and the complex permittivity of the silicon material is $\varepsilon=11.6 + 0.1i$. In order to verify perfect reflection by Mie response of the structure, we used three-dimensional full-wave electromagnetic field simulation by finite integral method to accurately calculate reflection and near-field distribution. In simulations, the x - and y -directions is set as periodic boundary conditions while open boundary condition is used for $\pm z$ directions. When

polarization angle is $\theta=90^\circ$ (the electrical field pointing in y direction), the simulation reflections as a function of grating thickness h and width x are shown in Fig. 1(b)(c). Each silicon grating line has a fixed period of $120\ \mu\text{m}$, various thickness h ranging from 60 to $120\ \mu\text{m}$ and width x changing from 40 to $60\ \mu\text{m}$. But it can be found that the perfect reflection can be achieved only at some single

frequency points. In contrast, when polarization angle is $\theta=0^\circ$ (the electrical fields pointing in x direction), Fig. 1(d)(e) show the reflection spectra with changing grating thickness h and width x , demonstrating perfect reflection at two frequencies. In a word, ultrabroadband perfect reflection can not be easily realized by common Si grating.

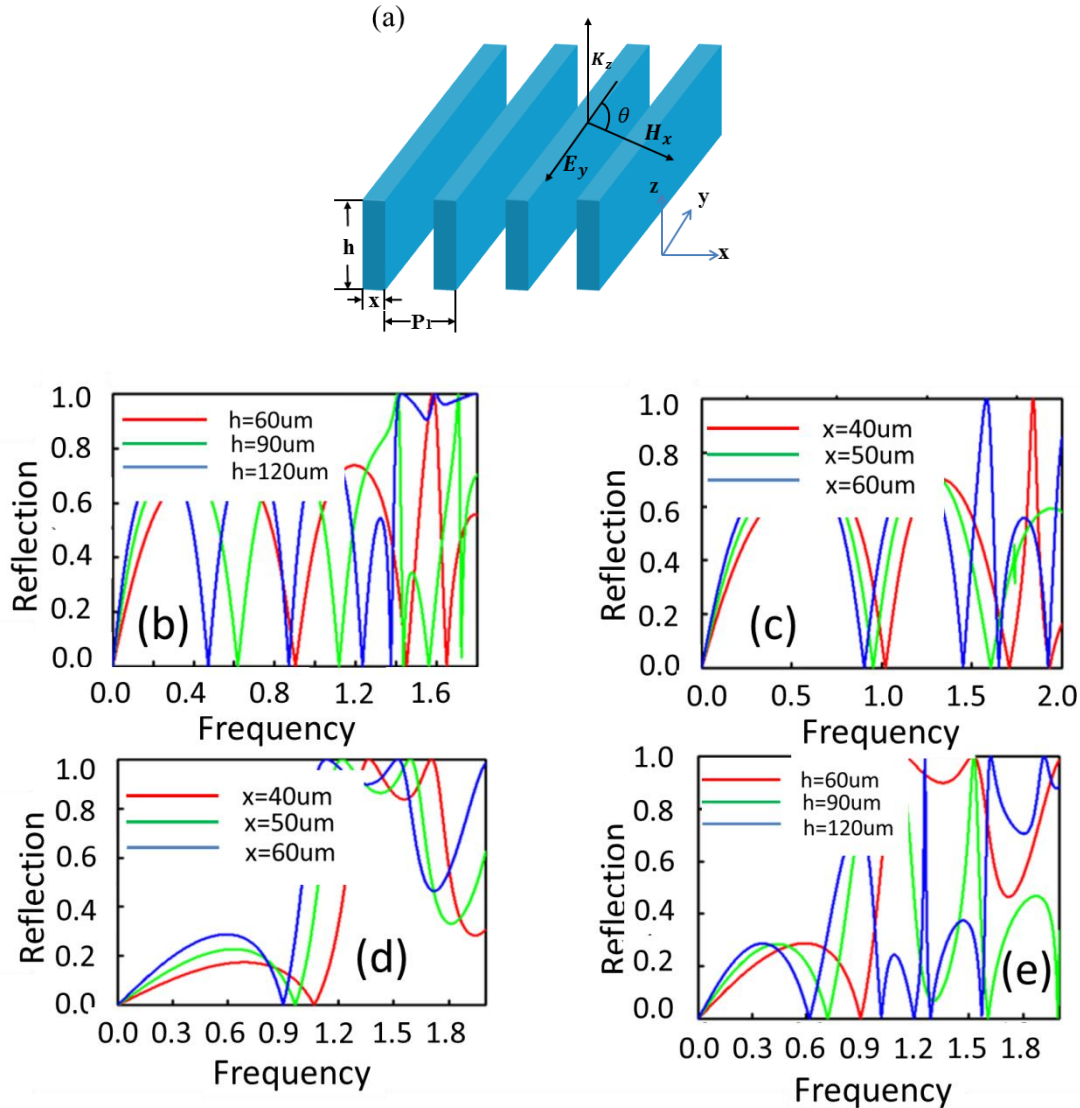


Fig. 1. (a) Schematic of common Si grating with height h and width x , the periodicity of the grating is P_1 . (b)(c) Dependent reflection for TE polarization. (d)(e) Reflection curves under different geometrical parameters of Si grating height h and width x for TM polarization

In order to realize an broadband perfect reflector, we propose a single layer super cell Si grating MM with two Si grating line in single unit cell as shown in Fig. 2(a). It can achieve ultrabroadband perfect reflector by adjusting the width of two Si grating line. The super cell of designed grating MM is of $p=120\ \mu\text{m}$, and the grating MM was optimized for these two grating lines in super cell with the width of $x_1=50\ \mu\text{m}$, $x_2=10\ \mu\text{m}$, $L=30\ \mu\text{m}$. The thickness of grating MM is of $h=60\ \mu\text{m}$. In simulations, the incident electric field is polarized along y axis. A peak reflection of

99.99% at 1.2THz and another peak reflection of 99.76% at 1.85 THz are shown in Fig. 2(b). Fig. 2(c)(d) illustrate the properties of single-negative all dielectric grating MM. The $\mu' < 0$ and $\epsilon' > 0$ between 1.23 THz and 1.62THz, and $\epsilon' > 0$ and $\mu' < 0$ between 1.19THz and 1.98 THz are demonstrated. The properties of effective constitutive parameters satisfy the first requirement of perfect reflection in Eq. (4). We also find in the same band that an extreme impedance mismatch is revealed with effective z' close to zero. It is obtained that near-perfect reflection

band of 0.79THz with reflection (>99%) from 1.19THz to 1.98THz can be realized. There is also a slight dip in the middle of the reflection band, and this dip can be

understood by the fact that this region is far from either resonances. Thus, an ultrabroadband perfect reflector can be achieved by super cell grating MM.

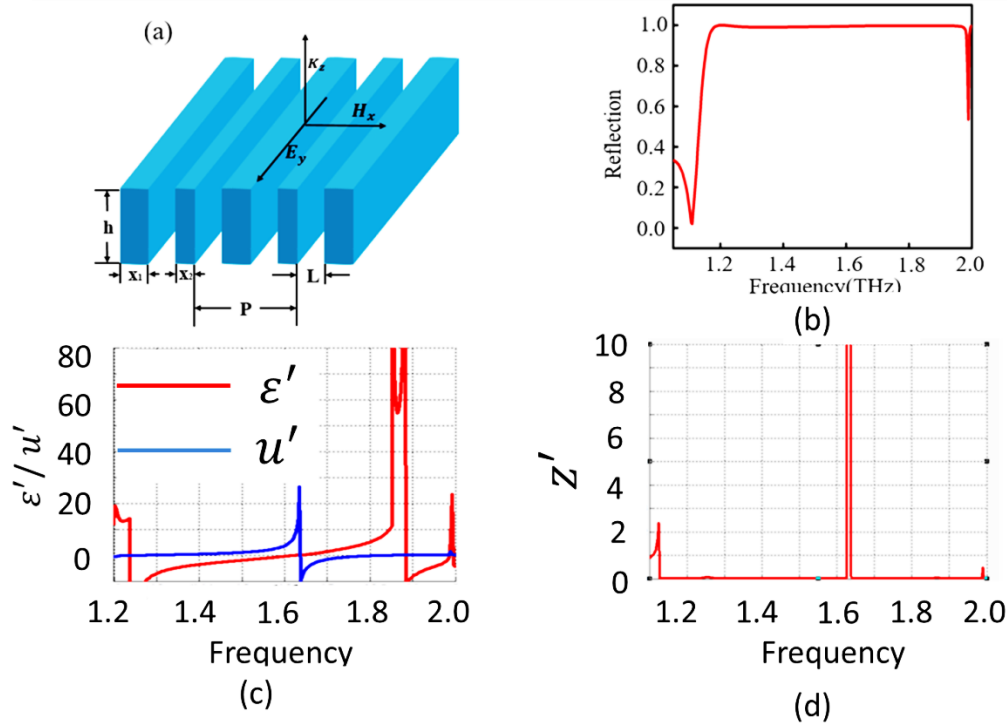


Fig. 2. (a) Schematic of proposed super cell grating MM. (b) Ultrabroadband perfect reflection by both electric and magnetic dipole resonances of MM at normal incidence. (c) Extracted real parts of effective permittivity and permeability for dielectric MM. (d) Retrieved impedance z' for super cell grating MM

To further characterize the coupling effects of perfect reflection on the resonance frequencies and get insight of physic mechanism, we investigate the distribution of electric fields and magnetic fields at the resonant frequencies of 1.2THz and 1.85THz, respectively. In Fig. 3, it is found that the strong electric field is distributed in the central region of the grating at 1.2THz, and a strong magnetic field at its cross section (x-z plane) is induced by the large displacement current. This is same as the conductive current in Ampere's law, which can be equivalent to two straight current wire and the

electromagnetic coupling between two electrical resonances [28,29] as indicated in Figs. 3(a) and 3(c). In Fig. 3(b)(d), two strong electric fields along $\pm y$ directions build up at the lateral sides of the second grating line. Meanwhile, two magnetic loops appear at y-z plane, which can be equivalent to two parallel current wires, and the first grating line ($x_1=50\mu\text{m}$) exists a strong magnetic resonance (TM₀₁ δ) with a weak electric resonance (TE₀₁ δ) [30], which give rise to artificial perfect electric and magnetic conducting conditions, respectively.

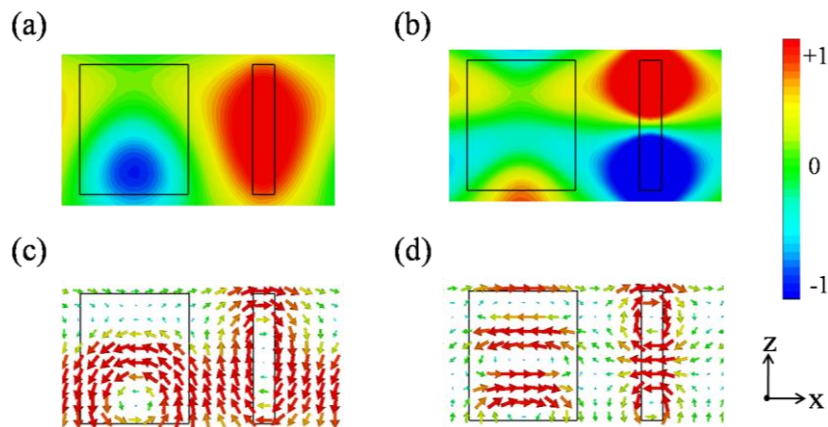


Fig. 3. Electric field ((a)–(b)) and magnetic field ((c)–(d)) distributions in super cell Si grating MM in unit cell at the frequencies of 1.2THz and 1.85THz, respectively

There is no doubt that this ultrabroadband perfect reflector is the simplest super cell Si grating structure, which can be easily fabricated by using lithography patterning or atomic layer deposition technology [31-34]. Furthermore, when we change the grating width x_2 ranging from $10\ \mu\text{m}$ to $40\ \mu\text{m}$, the perfect reflection bandwidth in Fig. 4(a) is decreased because of the electric response showing the blue-shift behavior. From Fig. 4(b)

with P varying from $120\ \mu\text{m}$ to $150\ \mu\text{m}$ without changing other parameters, it is interesting to note that the coupling effect of resonances (TE modes) is decreased with increasing the area of the air. TE mode is defined as the electric field vector parallel to grating groove. The corresponding frequency of dips is of blue-shift. The bandwidth of perfect reflection is slightly changed, but there is a reflection dip in broadband reflection.

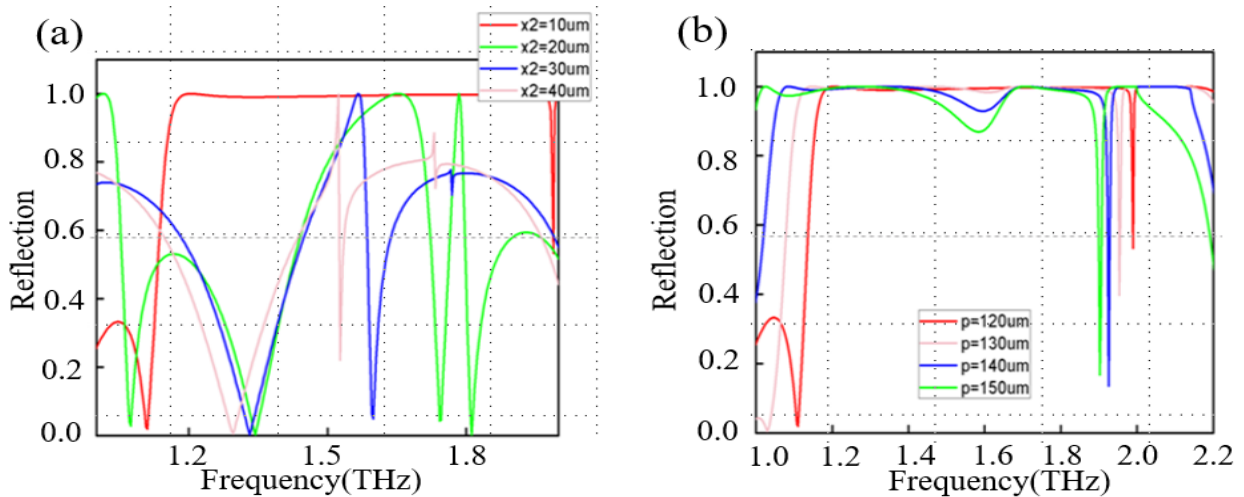


Fig. 4. (a) Reflection for the super cell grating MM with different width x_2 . (b) Reflection with different periods

In order to demonstrate the polarization effect of super cell grating MM in perfect reflection, TM mode terahertz wave is incident on MM. TM mode is defined as the electric field vector perpendicular to grating groove. To clearly identify the resonant frequencies, the transmission of super cell grating MM is demonstrated in Fig. 5. It can be found that polarization-dependent reflection characteristic of super cell grating is revealed. For TM mode, the electromagnetic field distribution at the resonant frequencies of $1.227\ \text{THz}$ and $1.599\ \text{THz}$, respectively, is numerically simulated in Fig. 6. It can be found that the strong field occurs in larger grating line x_1 , thus the resonant characteristics are dependent on the first grating line for TM mode. It can be obtained that the electric dipole resonance can be excited at $1.227\ \text{THz}$, and the magnetic dipole resonance can be motivated at $1.599\ \text{THz}$.

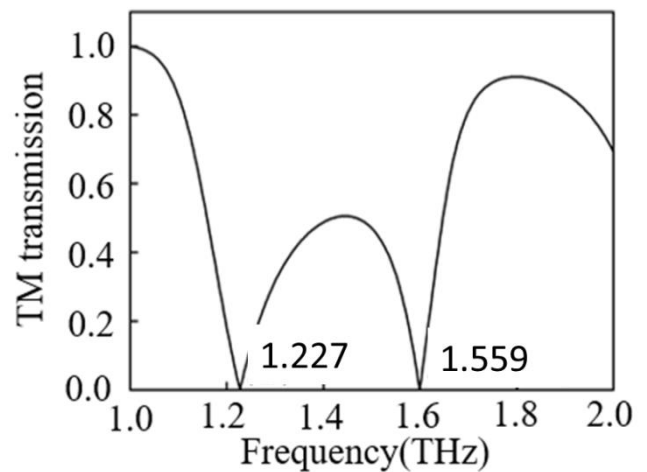


Fig. 5. Transmission for TM mode

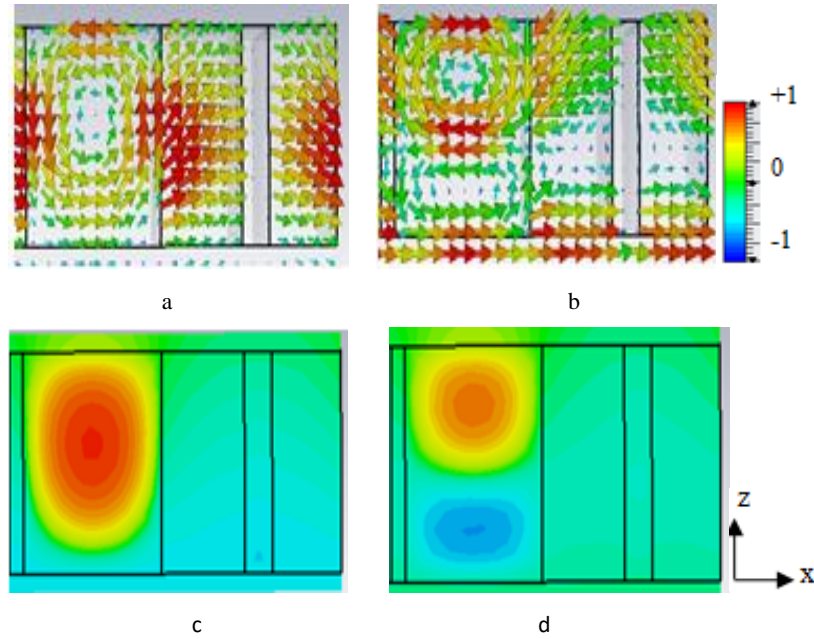


Fig. 6. (a) (b) electric field distribution and (c) (d) magnetic field distribution at the resonant frequencies of 1.227THz and 1.599THz, respectively, for TM mode

4. Super cell grating MM with multiple strips

Next, we will attempt realize broadband perfect reflector by super cell grating MM with three grating strips in one unit cell. Fig. 7(a) shows super cell grating MM with three grating strips in unit cell. After optimization, the broadband perfect reflection can be obtained with $P=120\mu\text{m}$, $L_1=25\mu\text{m}$, $L_2=45\mu\text{m}$, $x_1=50\mu\text{m}$, $x_2=10\mu\text{m}$, $x_3=5\mu\text{m}$ for TE mode in Fig. 7(b). From 1.75THz to

1.9THz, the reflection with near 100% can be achieved. But, there is a dip in reflection band at about 1.94THz. This transmission dip may be attributed to the resonance coupling effect of electric resonance and magnetic resonance. The effective constitutive parameters were also extracted in Fig. 7(c) and (d), and there results conform to the conditions of perfect reflector. Our design ideas can be applied to other fields in optical devices to realize broadband performance [35-44].

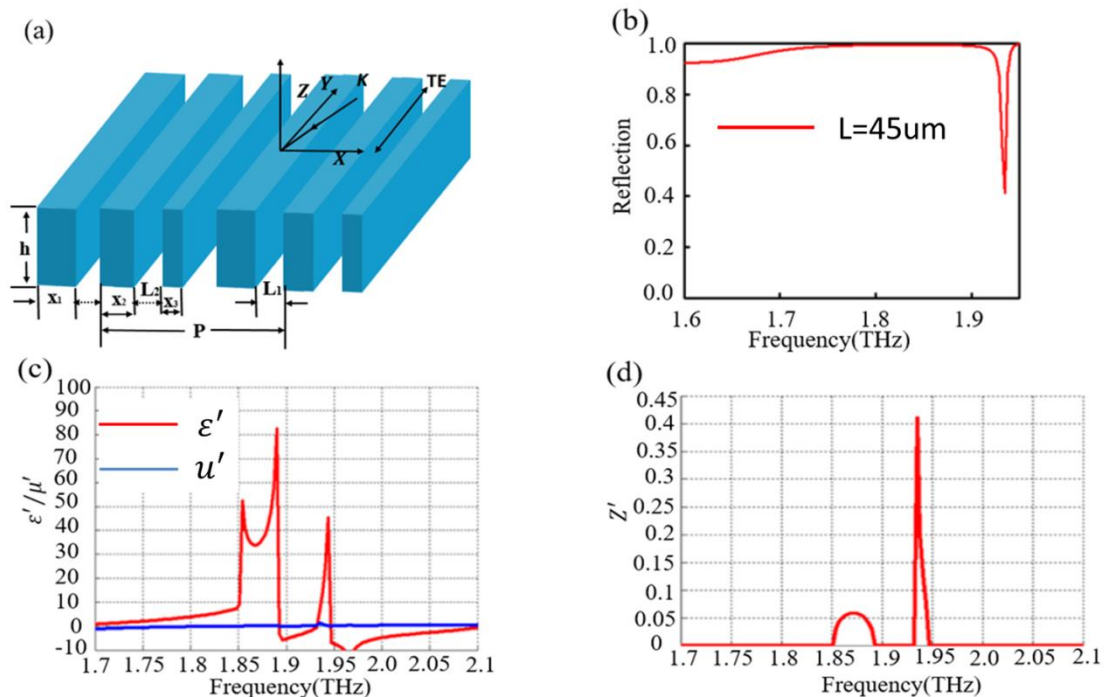


Fig. 7. (a) Schematic of proposed super cell grating MM with three strips in unit cell. (b) broadband perfect reflection by both electric and magnetic dipole resonances of MM at normal incidence. (c) Extracted real parts of effective permittivity and permeability for dielectric MM. (d) Retrieved impedance z' for super cell grating MM

5. Conclusions

In summary, we have demonstrated near-perfect reflection can be realized by electric and magnetic dipole Mie resonance in a single layer of one dimensional Si grating MM. Using finite-element analysis and realistic materials properties, we achieve an in-depth understanding of the physical mechanisms of the fundamental Mie resonances excited in both magnetic and electric modes in 1D dielectric grating. Then we proposed an ultrabroadband perfect reflector by super cell MM with two subcell Si grating lines with different width in unit cell. The band width of 0.79THz with reflection (>99.9%) from 1.19THz to 1.98THz in terahertz region can be realized. Also, the super cell grating MM with three grating strips in unit cell is designed to achieve broadband perfect reflection.

Acknowledgment

The authors acknowledge the support from National Key R&D Program of China (2018YFF01013005), Natural Science Foundation of Zhejiang Province (LY17F050009), National Natural Science Foundation of China (NSFC) (No. 61875159, No.61405182).

References

- [1] A. Ahmadi, H. Mosallaei, *Physical Review B* **77**(4), 5104 (2008).
- [2] Changcheng Xiang, Changhe Zhou, Wei Jia, Jun Wu, *Chinese Optics Letters* **16**(7), 070501 (2018).
- [3] C. M. Soukoulis, M. Wegener, *Nature Photon.* **5**, 523 (2011).
- [4] Eesa Rahimi, Kürşat Şendur, *Photonics Research* **6**(5), 427 (2018).
- [5] M. S. Wheeler, J. S. Aitchison, M. Mojahedi, *Phys. Rev. B* **73**(4), 045105-1 (2006).
- [6] S. W. Kim, B. W. An, E. Cho et al., *Nano Letters* **18**(6), 3865 (2018).
- [7] A. Grbic, G. V. Eleftheriades, *Physical Review Letters* **92**(11), 117403 (2004).
- [8] S. Morawiec, M. J. Mendes, S. Mirabella, F. Simone, F. Priolo, I. Crupi, *Nanotechnology* **24**(26), 265601 (2013).
- [9] V. V. Khardikov, E. O. Iarko, S. L. Prosvirnin, *J. Opt.* **12**(4), 045102 (2010).
- [10] Peng Cui, Wentao Zhang, Ying Song, *Chinese Optics Letters* **16**(11), 110603 (2018).
- [11] A. Boltasseva, H. A. Atwater, *Science* **331**(6015), 290 (2011).
- [12] N. I. Zheludev, *Science* **328**(5978), 582 (2011).
- [13] Z. Ma et al., *ACS Photon.* **3**(6), 1010 (2016).
- [14] Amir Ghobadi, Hodjat Hajian, Alireza Rashed Rahimi, Bayram Butun, Ekme1 Ozbay, *Photonics Research* **6**(3) 168 (2018).
- [15] J. Sautter et al., *ACS Nano* **9**(4), 4308 (2015).
- [16] R. Magnusson, M. Shokooch-Saremi, *Opt. Express* **16**(5), 3456 (2008).
- [17] B. Slovick, Z. G. Yu, M. Berding, S. Krishnamurthy, *Phys. Rev. B* **88**(16), 165116 (2013).
- [18] P. Moitra, B. A. Slovick, Z. G. Yu, S. Krishnamurthy, J. Valentine, *Appl. Phys. Lett.* **104**(17), 171102 (2014).
- [19] Tang, Yiqiao, A. E. Cohen, *Phys. Rev. Lett.* **104**(16), 163901 (2010).
- [20] A. Arbabi, E. Arbabi, H. Yu, S. M. Kamali, A. Faraon, *Nature Photon.* **11**(7), 415 (2017).
- [21] A. B. Evlyukhin et al., *Nano Lett.* **12**(7), 3749 (2012).
- [22] Q. Zhao, J. Zhou, F. Zhang, D. Lippens, *Mater. Today* **12**(12), 60 (2009).
- [23] X. Chen, T. M. Grzegorzczak, B.-I. Wu, J. Pacheco Jr., J. A. Kong, *Phys. Rev. E* **70**(1), 016608 (2004).
- [24] M. S. Wheeler, J. S. Aitchison, M. Mojahedi, *Phys. Rev. B* **72**(19), 193103-1 (2005).
- [25] D. R. Smith, S. Schultz, P. Markoš, C. M. Soukoulis, *Phys. Rev. B* **65**(19), 95104-1 (2002).
- [26] D. R. Smith, D. C. Vier, T. Koschny, C. M. Soukoulis, *Phys. Rev. E* **71**, 036617-1 (2005).
- [27] M. Choi et al., *Nature* **470**(7334), 369 (2011).
- [28] L. Lin et al., *Appl. Phys. Lett.* **108**(17), 1902-1 (2016).
- [29] A. Jain, P. Moitra, T. Koschny, J. Valentine, C. M. Soukoulis, *Adv. Opt. Mater.* **3**(10), 1431 (2015).
- [30] L. Lin et al., *Appl. Phys. Lett.* **108**(17), 1902-1 (2016).
- [31] Xi He, Cheng Liu, Jianqiang Zhu, *Chinese Optics Letters* **16**(9), 091001 (2018).
- [32] Jinhua Li, Xiangdong Zhang, *Photonics Research* **6**(6), 630 (2018).
- [33] K. Khairi, H. Kok Fong, Z. Lambak, M. I. Abdan et al., *Chinese Optics Letters* **16**(4), 040607 (2018).
- [34] Y. D. Peng, Z. J. Zhang, X. Q. Wang, S. D. Liu, A. H. Yang, X. S. Wang, *Optical and Quantum Electronics* **50**(8), 311 (2018).
- [35] X. Jing, X. Gui, P. Zhou, Z. Hong, *Journal of Lightwave Technology* **36**(12), 2322 (2018).
- [36] R. Xia, X. Jing, X. Gui, Y. Tian, *Optical Materials Express* **7**(3), 977 (2017).
- [37] X. Gui, X. Jing, Z. Hong, *IEEE Photonics Technology Letters* **30**(10), 923 (2018).
- [38] X. Jing, Q. Ye, Z. Hong, D. Zhu, G. Shi, *Superlattices & Microstructures* **111**, 830 (2017).
- [39] X. Bie, X. Jing, Z. Hong, C. Li, *Applied Optics* **57**(30), 9070 (2018).
- [40] X. Gui, X. Jing, P. Zhou, J. Liu, Z. Hong, *Applied Physics B* **124**(4), 68 (2018).
- [41] X. Gui, X. Jing, J. Liu, P. Zhou, Z. Hong, *Infrared Physics & Technology* **89**, 174 (2018).
- [42] J. Zhao, X. Jing, W. Wang, Y. Tian, D. Zhu, G. Shi, *Optics & Laser Technology* **95**, 56 (2017).
- [43] X. Jing, X. Gui, P. Zhou, Z. Hong, *IEEE Photonics Journal* **9**(1), 5900107 (2017).
- [44] J. Mian, H. Zhu, D. Zhu, et al., *Optoelectron. Adv. Mat.* **11**(3-4), 148 (2017).

#Corresponding author: jingxufeng_1984@163.com
*lichenxiacjlu@163.com